

**STUDY ON RADIOACTIVITY IN HUMAN TEETH,
ANIMAL BONES AND SOIL IN SELECTED AREAS IN
NORTHERN REGION OF MALAYSIAN PENINSULAR**

by

BASIM ABD ALHASSEN ABD ALHUSSEIN ALMAYAHI

**A thesis submitted in fulfillment of the requirements for the degree of Doctor of
Philosophy**

March 2013



قُلْ لَوْ كَانَ الْبَحْرُ مِدَادًا لِكَلِمَاتِ رَبِّي لَنَفِدَ الْبَحْرُ قَبْلَ أَنْ تَنْفَدَ كَلِمَاتُ رَبِّي وَلَوْ جِئْنَا بِمِثْلِهِ مَدَدًا

صدق الله العلي العظيم

"If the ocean were ink (wherewith to write out) the words of my Lord, sooner would the ocean be exhausted than would the words of my Lord, even if we added another ocean like it, for its aid"

“Kalaulah semua jenis lautan menjadi tinta untuk menulis kalimah-kalimah Tuhanku, sudah tentu akan habis kering lautan itu sebelum habis kalimah-kalimah Tuhanku, walaupun Kami tambahi lagi dengan lautan yang sebanding dengannya, sebagai bantuan”

AL-KAHF: 109

DEDICATION

To my father, mother, brothers, and sisters

ACKNOWLEDGMENTS

“Thankful to Allah”

This work was conducted in the School of Physics, Universiti Sains Malaysia. I would like to thank and wish to express my deep gratitude to my Main Supervisor, Professor Dr. Abd Aziz Tajuddin and Co-Supervisor Professor Dr. Mohamad Suhaimi Jaafar for their unlimited guidance, and encouragement throughout the period of this research. I am grateful for their excellent paternal affection and wonderful attitude. I cannot even offer them what they gave me to achieve this success, therefore I will make “doa” for them and remember them in my daily prayers.

I would also like to thank Associate Professor Dr. Sabar Bauk and Dr. Azahar Abdul Rahman for giving me access to use the HPGe and NaI (TI) spectrometers in the Biophysics Laboratory. Furthermore, I would like to thank Medical Physics Laboratory assistance Mr. Yahya Ibrahim, Biophysics Laboratory assistance Mr. Azmi Abdullah, Director General of Geological Survey, the Director General of Agriculture, the Director General of Penang Geographic Information System, Malaysia, all dental clinic directors involved in the sampling, the dentists, and nurses who helped and cooperated in collecting the teeth samples from the patients. Also I am very grateful to Universiti Sains Malaysia for providing a research grant 1001/PFIZIK/844085.

TABLES OF CONTENT

Acknowledgments	iv
Tables of Content	v
List of Tables	ix
List of Figures	xiv
List of Abbreviations	xix
List of Symbols	xx
Abstrak	xxiii
Abstract	xxv
CHAPTER 1 : INTRODUCTION	1
1.1 Background	1
1.2 Problem Statements	8
1.3 Objectives of the Thesis	8
1.4 Scope of the Study	9
1.5 Thesis Structure	9
CHAPTER 2 : THEORETICAL PART AND LITERATURE REVIEW	10
2.1 Theoretical Part	10
2.1.1 Electromagnetic Radiation	10
2.1.2 Radioactivity	10
2.1.3 Radiation Exposure and Dose	11
2.1.4 Natural Radioactivity	12
2.1.5 Environmental Radioactivity	12
2.1.6 Terrestrial and Aquatic Pathways	13

2.1.7 Food Chain from Soil to Humans	13
2.1.8 Transport of Soil Particles by Erosion	13
2.2 Literature Review	16
2.2.1 Natural Radioactivity Measurements of Gamma-Ray in Soil, Sand, and Water Samples	16
2.2.2 Radon and Thoron Measurements in Soil and Sand Samples by CR- 39 and RAD7 Detection	24
2.2.3 Natural Gamma-Ray Radioactivity Measurements for Bone Samples	27
CHAPTER 3 : STUDY AREA, MATERIALS, EQUIPMENTS, AND	29
METHODS	
3.1 Introduction	29
3.2 Study Area	29
3.3 Materials, Equipments, and Methods	36
3.3.1 Sample Collection, Preparation, and Measurements for Soil, Sand, and Water Samples using Gamma Spectroscopy	48
3.3.1.1 Global Positioning System (GPS)	50
3.3.1.2 Earth Drill Auger	51
3.3.1.3 Oven	52
3.3.1.4 Sieve and Mortar	52
3.3.1.5 Mechanical Balance, Marinelli Beaker	52
3.3.1.6 HPGe Detector and Lead Shielding	53
3.3.1.7 Liquid Nitrogen and Dewar	55
3.3.1.8 High Power Supply and Amplifiers	56
3.3.1.9 Energy Calibration	56
3.3.1.10 Absolute Efficiency	57

3.3.1.11 Energy Resolution	58
3.3.1.12 NaI (Tl) Detector and Lead Shielding	59
3.3.1.13 High Power Supply and Amplifiers	60
3.3.1.14 Absolute Efficiency and Energy Resolution	60
3.3.1.15 Multichannel Analyzer and Software	61
3.3.1.16 pH Meter	63
3.3.1.17 Gamma-Ray Transitions	63
3.3.1.18 GR-135 Spectrometer	64
3.3.2 <i>In Situ</i> Soil Radon Measurements in the Study Area by CR-39 Detection	67
3.3.2.1 CR-39 Plastic Track Detector (Radon Dosimeter)	68
3.3.2.2 PVC Cylinder	69
3.3.2.3 Chemical Etching, Water Bath, and Microscope with Software	69
3.3.2.4 Calibration	72
3.3.3 <i>In Situ</i> Soil Radon and Thoron Measurements in the Study Area by RAD7 Detection	73
3.3.3.1 RAD7 Solid-State Detector	75
3.3.4 <i>In Situ</i> Soil Surface Radon Measurements in the Study Area by Continuous Radon Monitoring	77
3.3.5 Tooth and Bone Samples from the Study Area	78
3.3.6 Calculations	85
3.3.6.1 Activity Concentration	85
3.3.6.2 Hazard Indices: Radium Equivalent Activity (Ra_{eq}), External Hazard Index (H_{ex}), Internal Hazard Index (H_{in}), Air-Absorbed Dose Rates (D_R), Annual Gonadal Dose Equivalent ($AGDE$) and Annual Outdoor Effective Dose Equivalent (H_R)	86

3.3.6.3 Statistical Analysis	88
CHAPTER 4 : RESULTS AND DISCUSSIONS	89
4.1 Soil and Sand from Penang	89
4.2 Soil Samples from Perlis, Kedah, and Perak	99
4.3 Water Samples from Penang, Perlis, Kedah, and Perak	110
4.4 Fieldwork Dose Measurements	117
4.4.1 Soil Types and Distribution of Gamma-Ray Dose Rates	119
4.4.2 Geological Types and Gamma-Ray Dose Rate Distribution	123
4.5 Soil Radon in the Study Area Using CR-39	130
4.6 Soil Radon and Thoron Measurements in the Study Area by RAD7 and SNC Detection	131
4.7 Teeth and Bone Samples from the Study Area	140
CHAPTER 5 : CONCLUSIONS AND FUTURE STUDIES	155
1.1 Conclusions	155
1.2 Future Studies	160
REFERENCES	161
APPENDIX	182
LIST OF PUBLICATIONS	196

LIST OF TABLES

Table 3.1	Geographic site of sampling points	36
Table 3.2	Information on soil samples from study area	39
Table 3.3	Geographic site of dental clinics in study area	45
Table 3.4	Geographic site of water samples	49
Table 3.5	Gamma transitions used to measure the activity concentrations of radionuclides using HPGe and NaI (Tl) detectors	64
Table 3.6	Information about the donor of teeth from the study area	81
Table 3.7	Information about bone samples from the study area	83
Table 4.1	Comparison of gamma-ray activity concentrations (Bq kg^{-1}) of sand samples with the values reported for other countries of the world	93
Table 4.2	Radium Equivalent Activity (Bq kg^{-1}), External and Internal Hazard Indices, Dose Rate (nGy h^{-1}), Annual Effective Dose (mSv y^{-1}), Annual Gonadal Dose Equivalent (mSv y^{-1}), $^{226}\text{Ra}/^{238}\text{U}$ and pH of the soil and sand samples in Penang state	94
Table 4.3	Radon concentration, temperature, pressure, and humidity for site surfaces using SNC monitor in Penang state	98
Table 4.4	Radiation Hazard Indices of soil samples of Perlis, Kedah, and Perak states	103
Table 4.5	Typical concentrations of K, U, and Th measured using GR-135 measured and Rn using SCN <i>in-situ</i> at 1 m above sampling sites in Perlis, Kedah, and Perak states	103

Table 4.6	Comparison of natural radioactivity levels in soil at different sites with those in other countries	108
Table 4.7	Radiation Hazard Indices of soil samples using a HPGe detector compared with the values reported from other countries	110
Table 4.8	Activity concentrations of natural radionuclides (Bq l^{-1}) in water samples	111
Table 4.9	Radiation Hazard Indices of water samples of Perlis, Kedah, and Perak states	112
Table 4.10	Activity concentrations of natural radionuclides (Bq l^{-1}) and Radiation Hazard Indices of water samples	113
Table 4.11	Comparison of gamma-ray activity concentrations (Bq kg^{-1}) of surface soil samples with the values reported for other countries of the world	114
Table 4.12	Soil group types and mean gamma-ray dose rate in study area	120
Table 4.13	Statistical summary and 95% confidence intervals for the mean gamma-ray dose rate for soil types	120
Table 4.14	Analysis of variance results of the dose rate for soil types	123
Table 4.15	Explanation geological features with a number of readings recorded	124
Table 4.16	Statistical summary and 95% confidence limit for the mean gamma-ray dose rate for geological types	125
Table 4.17	Analysis of variance results of the dose rate for geological types	127
Table 4.18	Statistical summary of the mean gamma-ray dose rates for soil and geological types	127
Table 4.19	Statistical summary and 95% confidence limit for the mean	128

	gamma-ray dose rate for each state	
Table 4.20	Analysis of variance results of the dose rate	128
Table 4.21	Comparison of soil ^{222}Rn concentrations with different countries	131
Table 4.22	Comparison of the surface air and soil gas ^{222}Rn and ^{220}Rn concentrations by Bq m^{-3} with previous measurements from different countries	140
Table 4.23	Summary statistics and 95% confidence intervals for mean radionuclides concentration for each age interval	146
Table 4.24	Significance of relationship of the radionuclides at different age intervals	148
Table 4.25	Analysis of variance results of the radionuclides concentrations for two genders	151
Table 4.26	Analysis of variance results of the radionuclides concentrations for smoker and non-smoker	151
Table 4.27	Statistical significance for the radionuclides concentrations in bones and teeth samples	154
Table A1	Specific activity (Bq kg^{-1}) of ^{40}K , ^{238}U series (^{226}Ra , ^{214}Pb , ^{214}Bi , ^{234}Th) and ^{232}Th series (^{228}Ac , ^{212}Bi , ^{212}Pb , ^{208}Tl)	182
Table A2	Typical concentrations of potassium, uranium, and thorium using GR-135 at 1 m above sampling site	184
Table A3	Analysis of variance results of radionuclide concentrations	184
Table A4	Radionuclides concentrations (Bq kg^{-1}) for sampling sites in the study area	185
Table A5	The gamma dose rates in the air in the study area are compared	185

with the values reported from other Districts in Malaysia and the World

Table A6	^{222}Rn concentrations in study area using CR-39	186
Table A7	Average (^{222}Rn and ^{220}Rn) concentrations, humidity, and temperature of the soil gas samples in study area using RAD7 at 50 cm depth	186
Table A8	Statistical summary and 95% confidence limit for the mean radon concentration for each state	187
Table A9	Analysis of variance results of radon concentration	187
Table A10	Average radon concentration, temperature, pressure, and humidity using the SNC monitor for all samples with accuracy $\pm 9 \text{ Bq m}^{-3}$ <i>in situ</i> for surface soil	188
Table A11	Analysis of variance results of radon concentration (SNC)	188
Table A12	Pearson's correlations matrix for ^{222}Rn and ^{220}Rn using RAD7 and SNC with meteorological parameters	189
Table A13	Estimated coefficients of linear equation between radon concentrations using RAD7 to ^{220}Rn , ASL, D_R , temperature (T), humidity (H%), and pressure (P)	189
Table A14	Estimated coefficients of linear equation between thoron concentrations to ASL, D_R , T, and P.	190
Table A15	Estimated coefficients of linear equation between radon concentrations using SNC to D_R , H, T, and P.	190
Table A16	Natural radionuclide concentrations (Bq g^{-1}) in teeth samples	190
Table A17	Estimated coefficients of linear equation between donor age and	193

radionuclides concentrations

Table A18	Pearson's correlations for the radionuclides concentrations with donor age	193
Table A19	Analysis of variance results of radionuclides concentrations for donor age intervals	193
Table A20	Natural radionuclide concentrations (Bq g^{-1}) in bone samples	194

LIST OF FIGURES

Figure 2.1	Main environment pathways of human radiation exposure	14
Figure 2.2	Production and release of ^{222}Rn	15
Figure 3.1	(a) a geological map of West Malaysia (b) the legend of map	32
Figure 3.2	A geographical map of West Malaysia and geological map of Penang state with sampling sites	34
Figure 3.3	(a) a soil map of West Malaysia and sampling sites (b) the legend of map	47
Figure 3.4	Global Positioning System (GPS)	51
Figure 3.5	Earth drill auger and PVC cylinder	51
Figure 3.6	Sieve and mortar	52
Figure 3.7	Mechanical balance	53
Figure 3.8	A typical Marinelli beaker filled with soil sample and sealed	53
Figure 3.9	High purity germanium (HPGe) spectroscopy set-up	54
Figure 3.10	Block diagram of the equipment set up of HPGe and NaI (Tl) spectrometers	55
Figure 3.11	HLC-Crystal	55
Figure 3.12	Typical spectrum after calibration with stripped gamma-ray background	57
Figure 3.13	Efficiency calibration curve for the HPGe detector	58
Figure 3.14	Determination of energy resolution for ^{60}Co (Present study)	59
Figure 3.15	Determination of energy resolution for ^{60}Co	59
Figure 3.16	Efficiency calibration curve for the NaI (Tl) detector	61
Figure 3.17	A typical soil spectra using MAESTRO software with 16,384 channels	62
Figure 3.18	(a) GR-135 with a sealed ^{137}Cs source: (b) GR-135 at 1 m from a soil surface	65

Figure 3.19	Gamma spectrum including the background counts for a sealed ^{137}Cs source of 9 kBq with 661.65 keV	66
Figure 3.20	Gamma spectrum measured by a GR-135 at 1 m above the soil surface	66
Figure 3.21	CR-39, cup, sponge, a double-sided tape, and iron rod	68
Figure 3.22	PVC cylinder with CR-39 chamber inside soil	69
Figure 3.23	Perforation CR-39 detector	70
Figure 3.24	CR-39 inside NaOH solution	70
Figure 3.25	Digital micrometer	71
Figure 3.26	Tracks density on CR-39 of two typical samples at depth of 50 cm for high and low radon concentrations	71
Figure 3.27	An optical microscope with software	71
Figure 3.28	CR-39 detector calibration	72
Figure 3.29	Preparation RAD7 with SNC and GR135 in fieldwork	74
Figure 3.30	RAD7 alpha spectrum	74
Figure 3.31	RAD7 analysis of ^{226}Ra source of time duration 4 days at room temperature. CAPTURE software has shown radon, temperature, and humidity lines.	76
Figure 3.32	(a) the radon concentration, temperature, pressure and humidity <i>in situ</i> for sample using a SNC monitor, (b) the window software used	78
Figure 3.33	Furnace for teeth samples	80
Figure 3.34	Mortar used to grind samples	81
Figure 3.35	Electrical balance	81
Figure 3.36	Furnace for bone samples	85
Figure 3.37	Mortar with bone samples	85
Figure 4.1	Portions of the gamma-ray spectra: (a) sample *135 of high	90

	concentration and (b) sample *074 of low concentration	
Figure 4.2	Concentration versus soil depth in Penang state: (a) Jelutong Apartments (b) Gertak Sanggul (c) Kg. Batu Feringhi (d) Kg. Sungai Burung (e) Balik Pulau (f) Penang Beach, Gurney (g) Kg. Pantai Acheh (h) Penang Hill (i) Kg. Teluk (j) Teluk Bahang (k) Guar Kepah (l) Taman Sentosa	92
Figure 4.3	Calculated versus measured dose rates (nGy h^{-1}) for soil samples in Penang state	97
Figure 4.4	Concentration versus soil depth in: (a) Kg. Pulau Chengai, Kedah (b) Kg. Lubok Peringgi, Kedah (c) Kg. Rama, Perlis (d) Bukit Ayer Kangar, Perlis (e) Kg. Telaga Baru, Kedah (f) Kg. Alor Radis, Perlis (g) Kg. Baru Padang Sanai, Kedah (h) Pulai, Kedah (i) Forest Research Complex, Perlis (j) Kg. Batu Enam, Perlis (k) Lebu Raya Grik, Perak (l) Kg. Bukit Sapi, Lenggong, Perak	101
Figure 4.5	Concentrations and dose rates for soil samples: (a) calculated versus measured dose rates, (b), (c), and (d) measured concentrations (^{40}K , ^{238}U , ^{232}Th , ^{226}Ra) using GR-135 and HPGe	105
Figure 4.6	Relation between radon and radium concentrations for soil sampling sites	106
Figure 4.7	Comparison between calculated concentrations of ^{40}K , ^{238}U , and ^{232}Th by HPGe spectroscopy (0 cm to 50 cm) and measured concentrations of ^{40}K , ^{238}U , and ^{232}Th by GR-135 spectrometer at a height of 1 m above sampling sites	107
Figure 4.8	^{210}Pb , ^{235}U , and ^{137}Cs concentrations from soil samples (0 cm to 10 cm) using HPGe spectroscopy	114
Figure 4.9	The gamma-ray spectra of two typical samples and NaI (Tl) detector	115

	calibration with MAESTRO software	
Figure 4.10	^{238}U , ^{232}Th , and ^{40}K concentrations of soil samples using NaI (Tl) spectroscopy	116
Figure 4.11	Efficiency of HPGe and NaI (Tl) detector as function of energy	116
Figure 4.12	Frequency histogram of gamma-ray dose rate for studies sites	117
Figure 4.13	Weibull probability plot of natural dose rate	118
Figure 4.14	Calculated gamma-ray dose rates in air of study area soils as compared with the values reported from districts and states in Malaysia and the world	119
Figure 4.15	Box chart showing the distribution and the variability of gamma-ray dose rate with soil type	122
Figure 4.16	Mean dose rate and 95% confidence interval with soil types	123
Figure 4.17	Box plot showing the distribution and the variability of gamma-ray dose with geological types	126
Figure 4.18	Mean dose rate and 95% confidence interval with geological types	126
Figure 4.19	Box plot showing the distribution and the variability of gamma-ray dose rate for each state	129
Figure 4.20	Mean dose rate for each state and 95% confidence interval for mean	129
Figure 4.21	Average ^{222}Rn concentrations vs. measurement sites	130
Figure 4.22	Average ^{222}Rn and ^{220}Rn concentrations measured using a RAD7 detector	132
Figure 4.23	Average ^{222}Rn concentrations using SNC	134
Figure 4.24	Average temperature and humidity for study area using RAD7 and SNC <i>in situ</i>	134
Figure 4.25	Relation between radon concentrations using RAD 7 for ^{220}Rn	135

	concentrations, ASL, and D_R	
Figure 4.26	Relation between radon concentrations using RAD 7 for a temperature (T), humidity (H%), and pressure (P)	136
Figure 4.27	Relation between thoron concentrations for ASL, D_R , T, and P	138
Figure 4.28	Relation between radon concentrations using SNC for D_R , H, T, and P	139
Figure 4.29	Correlation between donor age and radionuclides concentration	142
Figure 4.30	Average radionuclides concentrations versus age intervals (15-68 years)	144
Figure 4.31	Average radionuclides concentrations versus different age intervals	147
Figure 4.32	Average radionuclides concentrations of radionuclides in teeth samples as a function of gender (a) and males in relation to smoking (b)	150
Figure 4.33	Average radionuclides concentrations in animal bones and human teeth (a) and in study area (b)	153

LIST OF ABBREVIATIONS

<i>AGDE</i>	Annual Gonadal Dose Equivalent
ASL	Above mean sea level
B.G.	Number of counts for the background spectrum
<i>E.R.</i>	Energy Resolution
EPA	Environmental Protection Agency
FWHM	Full Width Half Maximum
Ge (Li)	Germanium Lithium doped
GPS	Global Positioning System
H.V.	High Voltage
HLC	Horizontal Level Cryostat
HPGe	High purity germanium
IAEA	International Atomic Energy Agency
ICRP	International Commission on Radiological Protection
LOAELs	Lowest-Observed-Adverse-Effect-Levels
<i>MDA</i>	Minimum Detectable Activity
MeV	Mega electron Volt
NaI (Tl)	Thallium doped Sodium Iodide
NPM	Northern Peninsular Malaysia
NORMs	Naturally Occurring Radioactive Materials
PEGIS	Penang Geographic Information System
ppm	part per million
PVC	Polyvinyl chloride
SC	Site Code
SI	International System of Unit
SNC	Sun Nuclear Corporation
SSNTD	Solid State Nuclear Track Detector
WHO	World Health Organisation

LIST OF SYMBOLS

${}^{219}_{86}\text{Rn}$	Actinon
${}^{220}_{86}\text{Rn}$	Thoron
${}^{222}_{86}\text{Rn}$	Radon
θ_c	Critical angle of etching
${}^{90}\text{Sr}$	Strontium
Ac	Actinium
Am	Americium
A_v	Avogadro's number
Bi	Bismuth
Bq	Becquerel
c	Light velocity
C	Coulomb
$\text{Ca}_{10}(\text{PO}_4)_6(\text{OH})_2$	Calcium hydroxyapatite
Ci	Currie
C_K	Activity concentration of ${}^{40}\text{K}$
Co	Cobalt
C_{Ra}	Activity concentration of ${}^{226}\text{Ra}$
C_{Rn}	Activity concentration of ${}^{222}\text{Rn}$
Cs	Caesium
C_{Th}	Activity concentration of ${}^{232}\text{Th}$
D_R	Air-absorbed dose rates
D_{Rc}	Calculated dose rate
D_{Rm}	Measured dose rate
E	Energy of gamma-ray photon
Eu	Europium
eV	electron Volt
Fe	Iron

Gy	Gray
h	Planck's constant
H_{ex}	External hazard index
H_{in}	Internal hazard index
H_R	Annual Outdoor Effective Dose Equivalent
h_t	Thickness
J	Joule
keV	kiloelectron Volt
kPa	Kilopascals
m	Mass
Mn	Manganese
M_o	Molecular weight
N	Normality
NaOH	Sodium Hydroxide
N_h	Number of hours
N_o	Activity of the source
p-value	Statistical significance
Pb	Lead
Po	Polonium
P_γ	Gamma-ray emission probability
Q_F	Quality factor
R	Rontgen
r	Correlation coefficient
Ra	Radium
Ra_{eq}	Radium equivalent activity
t	Exposure time for sample
$T_{1/2}$	Half-life of the radionuclide
t_c	Time of count
t_d	Decay time

t_e	Etching time
Th	Thorium
Tl	Thallium
t_o	Exposure time for standard source
U	Uranium
V	Ratio between track etching velocity to bulk etching velocity
V_B	Bulk etching velocity
V_T	Track etching velocity
V_w	Volume of distilled water
W	Weight of sample
W_{eq}	Equivalent weight of NaOH
W_N	Weight of NaOH
ε	Efficiency of detector
λ	Decay constant
λ_w	Wavelength of light
ν	Frequency
ρ	Tracks density of samples
ρ_o	Tracks density for standard source

KAJIAN RADIOAKTIVITI DALAM GIGI MANUSIA, TULANG HAIWAN DAN TANAH DI KAWASAN UTARA SEMENANJUNG MALAYSIA

ABSTRAK

Pengukuran radioaktiviti semula jadi bagi sampel tanah, pasir, dan air yang diambil di kawasan Utara Semenanjung Malaysia (Northern Peninsular Malaysia, NPM), iaitu yang terdiri daripada negeri Pulau Pinang, Kedah, dan Perak dijalankan dengan menggunakan spektroskop Exploranium GR-135 Plus, High Purity Germanium (HPGe), dan NaI (Tl). Kepekatan aktiviti ^{238}U , ^{232}Th , dan ^{40}K yang diperoleh di Pulau Pinang, Perlis, Kedah, dan Perak didapati berada dalam julat sebagaimana yang dilaporkan dalam literatur antarabangsa. Semua indeks bahaya kesihatan adalah di bawah nilai yang dicadangkan, kecuali bagi sesetengah tanah yang diambil di Kedah dan Perak. Tanah dengan H_{in} dan $H_{\text{ex}} < 1$ adalah sesuai untuk pertanian dan bahan binaan. Di samping itu, bagi air, H_{in} dan $H_{\text{ex}} < 1$. Oleh itu, air yang telah diproses dan dituras adalah selamat dan sesuai untuk kegunaan rumah dan industri. Tapak dengan kepekatan yang tinggi memaparkan ketidakseimbangan $^{226}\text{Ra}/^{238}\text{U}$. Tanah ^{235}U , ^{210}Pb , dan ^{137}Cs juga ditentukan dalam Bq kg^{-1} .

Jenis tanah dan maklumat geologi didapati mempengaruhi kadar dos sinar gama. Analisis ANOVA menunjukkan terdapatnya perbezaan yang signifikan dalam kadar dos sinar gama di antara jenis tanah dan geologi ($p < 0.001$). Taburan kadar dos adalah seperti berikut: Penang > Kedah > Perlis. Purata kepekatan radon *in situ* dan parameter meteorologi diukur dalam permukaan udara pada paras dasar dengan menggunakan pemantau atau monitor SNC. Kepekatan radon bagi pengukuran *in situ*

dalam gas tanah pada kedalaman sampel 50 cm dilakukan dengan menggunakan dua teknik yang berbeza, iaitu CR-39 dan RAD7.

Radionuklid semula jadi diukur dalam ekstrak gigi manusia dan tulang haiwan di negeri yang berbeza. Nilai radionuklid dalam gigi didapati berkurangan dalam urutan berikut: ^{40}K > ^{228}Ra > ^{226}Ra dan ^{210}Pb > ^{228}Th > ^{137}Cs . Korelasi positif yang signifikan pada $p < 0.01$ didapati di antara radionuklid dalam tulang dan gigi.

STUDY ON RADIOACTIVITY IN HUMAN TEETH, ANIMAL BONES AND SOIL IN SELECTED AREAS IN NORTHERN REGION OF MALAYSIAN PENINSULAR

ABSTRACT

Natural radioactivity measurements in soil, sand, and water samples obtained from Northern Peninsular Malaysia (NPM), comprising the states of Penang, Kedah, Perlis, and Perak were carried out using the Exploranium GR-135 Plus, High Purity Germanium (HPGe), and NaI (Tl) spectrometers. The activity concentrations of ^{238}U , ^{232}Th , and ^{40}K in Penang, Perlis, Kedah, and Perak states were found to be within those reported from literatures for other countries of the world. All the health hazard indices are well below their recommended value, except some soil from Kedah and Perak states. Soils with H_{in} and $H_{\text{ex}} < 1$ are suitable for agriculture and as building materials. Also, in this study H_{in} and $H_{\text{ex}} < 1$ for water, therefore, water after processing and filtration is safe and suitable for use in household and industrial purposes. The sites of high concentrations of displaying $^{226}\text{Ra}/^{238}\text{U}$ disequilibrium.

Soil ^{235}U , ^{210}Pb , and ^{137}Cs were also determined in Bq kg^{-1} . The soil types and geological formations influence gamma-ray dose rates. The ANOVA analysis indicates there are significant differences in gamma-ray dose rate between soil and geological types ($p < 0.001$). The distributions of the dose rate are as follows: Penang > Kedah > Perlis. The average *in situ* radon concentrations and meteorological parameters were measured in the surface air at the ground level using a SNC

monitor. Radon concentrations for *in situ* measurements in soil gases at a sampling depth of 50 cm were done using two different techniques are CR-39 and RAD7.

Natural radionuclides were measured in extracted human teeth and animal bones from people and animal living in different states. The values of radionuclides in teeth decreased in the order $^{40}\text{K} > ^{228}\text{Ra} > ^{226}\text{Ra}$ and $^{210}\text{Pb} > ^{228}\text{Th} > ^{137}\text{Cs}$. Significant positive correlations at $p < 0.01$ were found between the radionuclides in bones and teeth.

CHAPTER 1

INTRODUCTION

1.1 Background

Experimental studies on naturally occurring environmental radionuclides contribute to the current knowledge of geological processes and atmospheric phenomena. Environmental radionuclides can be divided into three groups: radionuclides of primordial origin, decay products of primordial radionuclides, and radionuclides generated by human activities. Radionuclides are commonly found in rocks, soil, and water that make up the planet, buildings, and homes. Soil is an important environmental material used as raw material and product for buildings, roads, playgrounds, and land filling. The functioning of terrestrial Earth systems continuously affects man and induced global changes. These effects are reflected by changes in the ecological functions of terrestrial systems such as surface water bodies (flood prevention), soils (fertility for food production), and groundwater (drinking water supply) (Froehlich, 2010). Contamination of land and water can result from deposition of waste material originally introduced into the atmosphere, discharge directly released into surface or subsurface waters, and wastes in or on the ground. The primary reason for this concern is that radioactive contamination of the environment may result in exposure of humans.

Groundwater or surface water erosion coupled to subsurface aquifers, soils, and the atmosphere may eventually mobilize ground contaminants. Atmospheric pollutants become deposited on soils or surface waters. The mechanisms for removing contaminants from soil involve transportation by water through a sequence of processes, including surface runoff and leaching into soil water that seeps into

streams. Humans are surrounded by natural radioactivity. Radioactive isotopes are present in human bodies, houses, air, water, and the ground (Eisenbud & Gesell, 1997; Henriksen & Maillie, 2003).

The study of natural radioactivity is important in understanding the behavior of natural radionuclides in the soil environment. Such information can be used as associated parameter values for radiological valuations (Vera *et al.*, 2003). ^{238}U and ^{232}Th chains, as well as ^{40}K dominate terrestrial radioactivity. Cosmic rays produce radioactive nuclei via their interactions with nuclei found in the atmosphere and the Earth's crust. Radiation exposure naturally varies with the environment depending on the concentration of radioisotopes present in the ground.

The average radiation exposure in Europe and the United States is 0.5 mSv y^{-1} (Gruppen, 2010). This dose may exhibit strong regional variations. Dose rates up to 18 mSv y^{-1} have been recorded in Germany's Black Forest region. The highest known exposure rates on Earth have been reported to occur in the following areas: Kerala, India with 26 mSv y^{-1} , Brazil on the Atlantic coast with up to 120 mSv y^{-1} ; and Ramsar, Iran with 450 mSv y^{-1} (Gruppen, 2010). The terrestrial radiation dose rate from gamma-rays emitted by naturally occurring radionuclides is influenced by soil types as well as geological and geographical conditions (Florou & Kritidis, 1992; UNSCEAR, 2000). Related literature on environmental terrestrial radiation indicates that further studied need to be conducted in Malaysia, especially in Penang, Perlis, Kedah, and the upper portion of North Perak in Northern Peninsular Malaysia (NPM). Several studies have been performed previously (Tajuddin *et al.*, 1994; Ramli, 1997; Ramli *et al.*, 2005a; Ramli *et al.*, 2005b; Omar *et al.*, 2006; Abdul Rahman & Ramli, 2007; Siak *et al.*, 2009; Ramli *et al.*, 2009a, 2009b).

Common long-lived radioactive elements such as uranium and thorium decay slowly to produce other radioactive elements, including radium, which undergo radioactive decay. ^{226}Ra is moderately soluble in water and can enter groundwater by dissolution of aquifer materials, desorption from rock or sediment surfaces, and ejection from minerals by radioactive decay. ^{226}Ra decays by alpha emission to the inert gas ^{222}Rn without color, odor, or taste. Within the U-Ra decay chain, radon is produced in almost every soil. Radon decays through a series of short-lived (^{218}Po , ^{214}Pb , ^{214}Bi , and ^{214}Po) and long-lived (^{210}Pb , ^{210}Bi , and ^{210}Po) isotopes and then stabilizes as ^{206}Pb . Atmospheric ^{210}Pb is mainly produced within the atmosphere by ^{222}Rn decay; the direct precursor of ^{210}Pb is ^{214}Po . Radon isotopes are members of the natural decay series: the ^{238}U decay series (^{222}Rn , $T_{1/2} = 3.8$ days), the ^{232}Th decay series (^{220}Rn , $T_{1/2} = 56$ s) and the ^{235}U decay series (^{219}Rn , $T_{1/2} = 3.9$ s).

As a natural radioactive noble gas, radon comes from water and soil and gets into the air. The amount of radon reaching the atmosphere close to the soil is determined by various factors such as soil type, concentration of its precursor ^{226}Ra in soil, and meteorological conditions such as temperature and precipitation. Natural environmental radioactivity due to gamma radiation depends on geological and geographical conditions and can be observed in various quantities in soils (UNSCEAR, 2000). ^{222}Rn gas concentration can vary according to geological and geographical locations. ^{222}Rn is continuously generated in the soil by the decay of natural ^{238}U , whereas ^{220}Rn results from the decay of natural ^{232}Th . Both ^{238}U and ^{232}Th are commonly found in soils and minerals. A much smaller fraction of the thoron gas in soil reaches the interior of a building. Despite this low quantity, thoron remains hazardous because its progeny includes ^{212}Pb , which has a half-life of 10.6 hours and is long enough to accumulate to significant levels in breathable air.

^{226}Ra and ^{228}Ra isotopes are considered the most important natural radionuclides of the ^{238}U and ^{232}Th series, respectively. The distributions for ^{238}U and ^{230}Th in bones are similar and have rather lower concentrations than ^{232}Th . These radioisotopes chemically and physiologically behave like calcium and tend to be concentrated in the bones and teeth (Dewit *et al.*, 2001).

In the physical environment, radioisotopes form soluble compounds and can contaminate underground reservoirs, soils, plantations, food sources and consequently, the human food chain. ^{226}Ra is a well-known “bone-seeking” radionuclide that accumulates in calcareous tissues because of its chemical similarity to calcium (Whicker & Schultz, 1982). The movement of ^{226}Ra through food chains is considered “moderate,” and 99% of the ^{226}Ra body content is in human bones (ICRP Committee II, 1960). ^{226}Ra is expected to be present in bone tissues because this radionuclide tends to be moderately transferable in the physical environment.

^{226}Ra is taken up by vegetation from the soil, and assimilated efficiently from the gut when ingested by animals (NCRP, 1999). The retention of ^{226}Ra in bones is high and accumulates over time under conditions of chronic intake. The levels measured in human bones from several urban locations have ranged from 0.03 Bq kg^{-1} to 0.37 Bq kg^{-1} (Eisenbud & Gesell, 1997).

Among the radionuclides derived from anthropogenic sources, ^{137}Cs is the major source but represents only between 2% and 3% of the total gamma-ray dose rate.

^{137}Cs is derived from land mammal consumption. Studies have shown that the distribution of ^{137}Cs in surface soils is attributed to differences in climate and topographical situations pertinent to a location (Tang *et al.*, 2002). The International Commission on Radiological Protection assumes that ^{137}Cs and ^{40}K are homogeneously distributed throughout the body of an organism. ^{137}Cs and ^{40}K are

generally not considered bone seekers; however, the accumulation of their radionuclides causes internal radiation exposure in humans and animals (Hong *et al.*, 2011).

Exposure to increased levels of radium for long periods can lead to death and severe health problems such as cancer (especially bone, liver, and breast cancer), anemia, fractured teeth and cavities, as well as cataracts.

Radium can replace calcium and enter the hydroxyapatite structure (Yamamoto *et al.*, 1994). The Chernobyl accident in 1986, along with other localized releases from various sources, contaminated the terrestrial and marine environment (Strand *et al.*, 2002). An indigenous population basically dependent on wildlife is vulnerable to radioactive exposure from ingestion of terrestrial and marine food (Cooper *et al.*, 2000; Macdonald *et al.*, 2007; Hamilton *et al.*, 2008). The uptake routes of ^{210}Pb and ^{226}Ra are through plants and from the soil, respectively (Pietrzak-Flis & Skowronska-Smolak, 1995). ^{238}U , ^{232}Th series, ^{40}K , and their daughters are the main contributors to internal radiological doses received by humans from natural radioactive sources.

Internal radiation dose varies with radionuclide concentration in air, soil, water, foodstuff, and rate of intake. This concentration differs from one human group to another. Therefore, radionuclides accumulated in teeth depend on the transfer rate of radionuclides from air, soil, and water to the teeth. ^{226}Ra uptake from public water supplies into teeth was studied as part of an evaluation of a radiological health problem (Samuels, 1964). The results of the study focused on radium metabolism as it relates to teeth (Samuels, 1966). Teeth are composed of several tissues: dentin, enamel, cementum, and pulp. Dentin, a highly sensitive calcified tissue, is the main core of each tooth. Dentine is covered with enamel on the crown portion and cementum on the roots.

^{222}Rn exposure is considered another potential source of increased ^{210}Po and ^{210}Pb in teeth because ^{210}Po occurs at the end of the ^{222}Rn decay chain. Clemente *et al.* (1982, 1984) found that incremental ^{210}Pb tooth content is due to excessive exposure to radon daughter in residents near Badgastein spa in Austria. Aghamiri *et al.* (2006) showed that the teeth of the inhabitants of Iran have more ^{226}Ra radioactivity concentration than those of the inhabitants of low-radiation areas because of higher ^{226}Ra content in soil and water.

Radionuclides concentrations in teeth are good indicators of radiation contamination in the human body. Teeth are used widely as markers of biological exposure to environmental pollution (Budd *et al.*, 1998; Appleton *et al.*, 2000; Carvalho *et al.*, 2000; Gomes *et al.*, 2004). However, studies on this subject are limited availability. A possible reason is that earlier investigators have assumed that the uptake and distribution of radionuclides in teeth are similar to those in bones. As such, these investigators have neglected the study of the distribution of radionuclides and the histopathologic changes in dental tissues.

In addition, analysis of teeth and bones may aid in the investigation of low dose and low dose-rate exposure of radionuclides potentially emitted throughout the process of nuclear energy production (Culot *et al.*, 1997) because the roots of teeth exhibit a bone-like structure (Gulson & Gillings, 1997). The literature review related to radionuclide concentration especially gamma activity concentration in teeth, indicates that further investigation has to be conducted.

1.2 Problem Statements

The problems are as follows:

1. What is the natural radionuclide concentration in the study area?
2. What is the correlation between the natural radionuclide concentration in teeth and that in bones?
3. What is the relationship between gamma-ray dose rate based on geology and that based on soil types in the study area?

1.3 Objectives of the Thesis

The objectives of this study are as follows:

1. To determine the quantity and quality of natural radioactivity from ^{226}Ra , ^{214}Pb , ^{214}Bi , ^{234}Th , ^{228}Ac , ^{212}Bi , ^{212}Pb , ^{208}Tl , and ^{40}K in soil, sand, water, ^{40}K , ^{137}Cs , ^{210}Pb , ^{226}Ra , ^{228}Ra , and ^{228}Th in human teeth, and animal bones, as well as to identify any radiological hazard in terms of absorbed dose rate in air and annual effective doses.
2. To compare the level of radionuclide concentration in the study area and examine the relationship between the radionuclide content in teeth and that in bones.
3. To determine the relationship between the gamma-ray dose rate based on geology and that based on soil types.

1.4 Scope of the Study

1. This study focuses on the natural radioactivity found in soil, sand, and water samples in the first phase of the study.
2. The second phase of the study concerns the natural radioactivity found in teeth and bone samples and the correlation between the two phases.

Samples collected from the study area were analysed using different detectors (HPGe, NaI (Tl), GR-135, RAD7, CR-39, and SNC 1029). Data analyses were performed using different software.

1.5 Thesis Structure

This thesis consists of five chapters. Chapter 1 comprises the introduction, problem statements, objectives of the thesis, scope of study, and the thesis structure. Chapter 2 contains the theoretical part and the literature review. Chapter 3 includes the study area, materials, equipments, and methods. Chapter 4 presents the results and discussions of this study.

Finally, Chapter 5 states the conclusions and provides suggestions for future research.

CHAPTER 2

THEORETICAL PART AND LITERATURE REVIEW

2.1 Theoretical Part

2.1.1 Electromagnetic Radiation

Electromagnetic radiation (uncharged radiation) includes X-ray emitted in the rearrangement of the electron shells of atoms, and the gamma-rays emitted from the transitions within the nucleus (Knoll, 2000).

Radiations such as alpha particles or low-energy X-rays only slightly penetrate a given thickness of material. Beta particles can penetrate more deeply than alpha particles and tolerate sources up to a few tenths of a millimeter in thickness. Hard radiations such as gamma-rays or neutrons are less affected by self-absorption and can tolerate sources up to millimeters or centimeters without seriously affecting the radiation properties (Knoll, 2000).

2.1.2 Radioactivity

The activities of radioisotope sources are represented by their rates of decay, given by the main law of radioactivity (Knoll, 2000)

$$\frac{dN_o}{dt_d} = -\lambda N_o \quad (2.1)$$

where N_o is the activity of the source, λ (s^{-1}) is the decay constant $= \frac{\ln 2}{T_{1/2}}$, $T_{1/2}$ is

the half-life of the radionuclide, and t_d is the decay time.

The unit of activity is expressed in the SI unit Becquerel (Bq), where $1 \text{ Bq} = 2.703 \times 10^{-11} \text{ Ci}$. The specific activity of radionuclides is defined as the activity per

unit mass of the radioisotope samples. This activity can be calculated as follows (Knoll, 2000):

$$\text{Specific Activity} = \frac{\text{Activity}}{\text{Mass}} = \frac{\lambda N_o}{(NM_o)/A_v} = \frac{\lambda A_v}{M_o} \quad (2.2)$$

where M_o = molecular weight and A_v = Avogadro's number (6.02×10^{23} nuclei per mole)

The electron volt (eV) is the traditional unit for measuring radiation energy. Multiples of electron volts, such as kilo electron volts (keV) and mega electron volts (MeV), are commonly used to measure the energy of ionizing radiation.

The SI unit of energy is the Joule (J), where $1 \text{ eV} = 1.602 \times 10^{-19} \text{ J}$, and the energy of a gamma-ray photon is (Knoll, 2000)

$$E \text{ (eV)} = h\nu = h \frac{c}{\lambda_w} \quad (2.3)$$

where h = Planck's constant ($4.135 \times 10^{-15} \text{ eV s}$), ν = frequency, c = light velocity, and λ_w = wavelength of light (meter) = $1240000/E$

2.1.3 Radiation Exposure and Dose

The concepts of radiation exposure and dose play primary functions in the measurement of personnel protection at radiation-producing facilities and medical applications for radiation. The unit of gamma-ray exposure is defined by the charge dQ because of the ionization electrons within a volume of air and mass dm . The exposure value is then equal to dQ/dm . The SI unit of gamma-ray exposure is coulomb per kilogram ($C \text{ kg}^{-1}$), and the historical unit is the Rontgen (R). The two units are related by (Knoll, 2000):

$$1 R = 2.58 \times 10^{-4} C kg^{-1}$$

The absorbed dose is defined as the energy absorbed from the radiation per unit mass of absorber, and the historical unit of absorbed dose is rad. The unit rad is gradually replaced by the SI unit gray (Gy), which is defined as 1 joule per kilogram. The two units are related as

$$1 Gy = 100 rad$$

2.1.4 Natural Radioactivity

All natural elements that have atomic numbers $Z > 82$ are emitters of radiation; ^{232}Th , ^{235}U , and ^{238}U series are the natural radioactive series. The ^{232}Th series begins with ^{232}Th nuclei and ends with ^{208}Pb . The ^{235}U series begins with ^{235}U nuclei and ends with ^{207}Pb , which is a stable element. The ^{238}U series begins with ^{238}U nuclei and ends with ^{206}Pb , which is a stable element.

2.1.5 Environmental Radioactivity

Experience with the dangers of radioactive materials preceded by discovery of the phenomenon by many years (Eisenbud & Gesell, 1997). The discovery of the radioactivity phenomenon led to testing of soil and water, which were then shown to contain high concentrations of natural radioactive elements. Radiation exposure varies with the environment depending on radioisotope concentrations (for example, ^{210}Pb , ^{137}Cs , ^{228}Th , ^{226}Ra , ^{228}Ra , ^{234}Th , ^{214}Pb , ^{214}Bi , ^{212}Pb , ^{212}Bi , ^{208}Ti , ^{235}U , and ^{40}K) in soil.

2.1.6 Terrestrial and Aquatic Pathways

Contamination in land and water is caused by deposition of waste materials originally introduced into the atmosphere, discharge of waste placed on the ground into surface or subsurface water waste placed on the ground, with ground contamination eventually mobilized by groundwater or erosion. Elements that are easily absorbed on sediments and suspended matter include Cs, Mn, Fe, Co, and the actinide elements.

2.1.7 Food Chain from Soil to Humans

Artificial radionuclides behave in a similar manner, and pollution of the food chain all over the world by radioactive elements produced during atmospheric nuclear weapon testing may have occurred during the past half-century. For example, ^{90}Sr and ^{137}Cs fallout from nuclear weapon testing in the upper 10 cm of soil was found to occur for the first few years after deposition (Eisenbud & Gesell, 1997).

2.1.8 Transport of Soil Particles by Erosion

Erosion by rainfall or runoff is one mechanism to transport of radionuclides inserted into the soil surface. Erosion by wind causes resuspension of pollutants that have settled on the surface. The suspended radionuclides settle on plants, water, and soil, and eventually enter the food chain. These radionuclides may be deposited on skin and clothing, allowing them access to the human body by inhalation and ingestion, or directly affect the human body by external exposure, as shown in Figure 2.1.

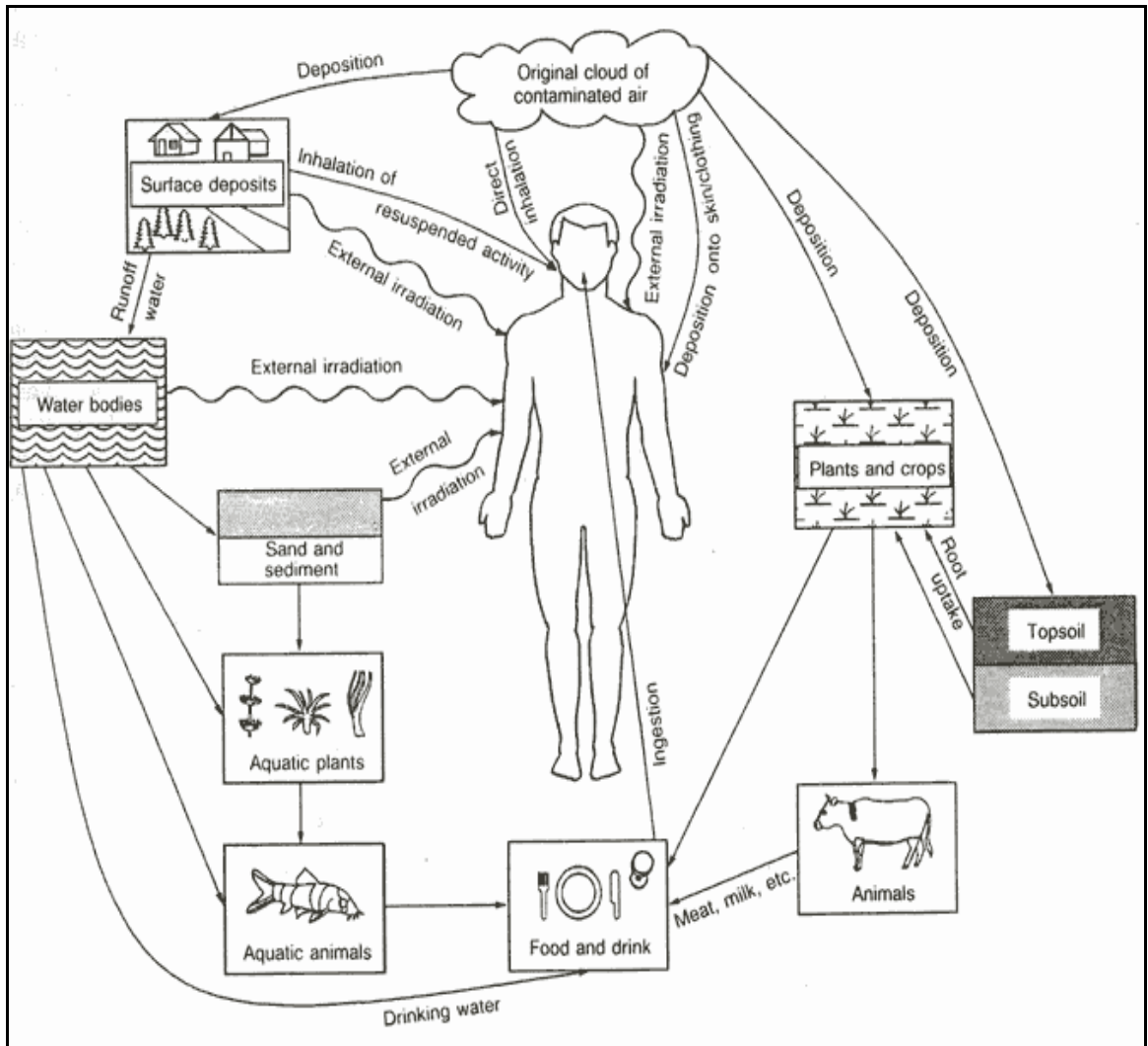


Figure 2.1: Main environment pathways of human radiation exposure (IAEA, 1991)

Natural radionuclides accumulate in the human body after intake through food, water, and air. The two main exposure pathways are inhalation and ingestion. Inhalation may be an important exposure pathway to the public. Ingestion of contaminated soil, water, and food can also lead to internal exposure. Radiation damage to the lung caused by inhalation of radon in air may increase the risk of cancer. Figure 2.2 shows the production of ^{222}Rn in the uranium–radium chain and the release of this gas through cracks in rocks or the ground into the air.

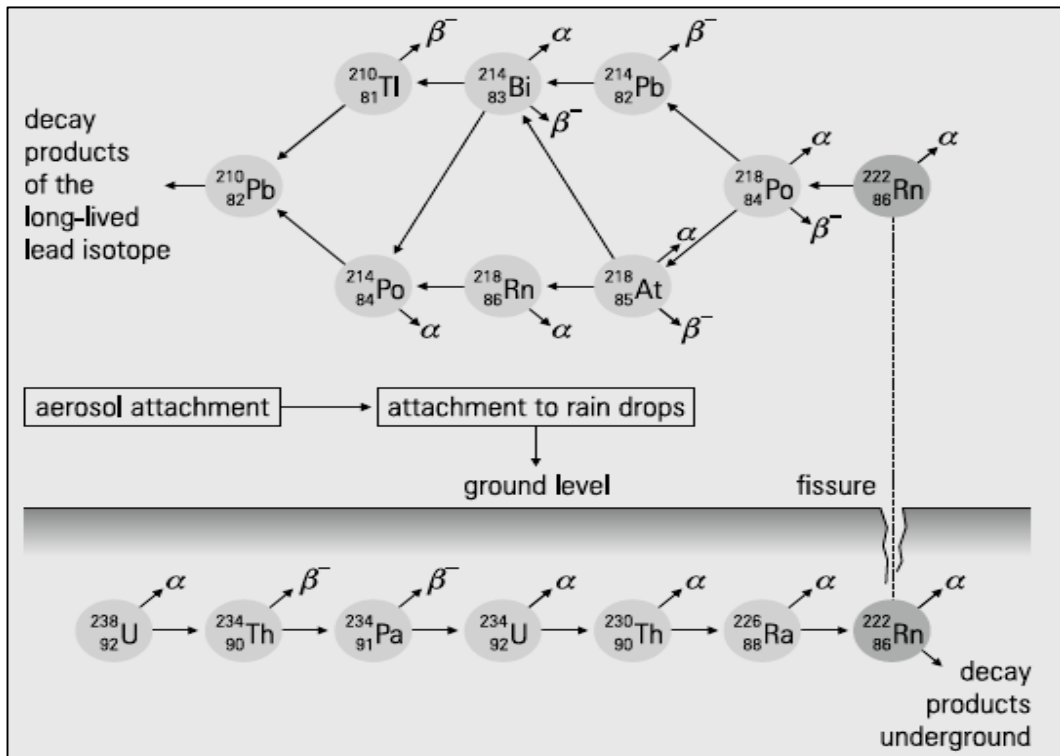


Figure 2.2: Production and release of ^{222}Rn (Gruppen, 2010)

2.2 Literature Review

2.2.1 Natural Radioactivity Measurements of Gamma-Ray in Soil, Sand, and Water Samples

Tajuddin *et al.* (1994) measured the natural radiation levels along the highway of Peninsular Malaysia by using a large NaI (TI) scintillation detector. The highest reading was in Bukit Merah ($1.5 \mu\text{Gy h}^{-1}$), whereas the gamma-ray levels around Penang (150 nGy h^{-1}) were found to be slightly higher than those in Kuala Lumpur (125 nGy h^{-1}). The levels in the southern part of Ipoh and its surrounding areas (40 nGy h^{-1}) were less than those for Georgetown and Kuala Lumpur.

Ramli (1997) studied the relationship of environmental terrestrial gamma-radiation dose with soil type in the Pontian District, Malaysia by using a NaI (TI) survey meter. The average value of the natural terrestrial gamma-ray dose in Pontian District was estimated to be 67 nGy h^{-1} .

Ramli *et al.* (2005a) measured the ^{238}U and ^{232}Th concentrations in the soil and water at Palong, Johor by using an HPGe detector and a NaI (TI) survey meter. The ^{238}U and ^{232}Th concentrations in the soil were determined to be 316 and 616 Bq kg^{-1} , respectively, whereas those in the water were found to be 8.37 and 1.57 mBq kg^{-1} , respectively. The gamma-ray dose rate in Bali Bandung Village, Malaysia was found to be 1440 nGy h^{-1} .

Ramli *et al.* (2005b) also studied the terrestrial gamma-radiation dose in Melaka state, Malaysia by using a NaI (TI) survey meter. The population-weighted mean dose rate throughout the Melaka state is 172 nGy h^{-1} .

Omar *et al.* (2006) measured the radiation levels on the roads in Peninsula Malaysia by using a NaI (TI) survey meter. The gamma-ray dose rate ranged from 36 nGy h⁻¹ to 1560 nGy h⁻¹.

Abdul Rahman & Ramli (2007) determined the terrestrial gamma-radiation dose rates as well as the concentration level of ²³⁸U and ²³²Th in the surface soil samples collected in Ulu Tiram, Malaysia by using an HPGe detector and a NaI (TI) scintillation survey meter. The ²³⁸U and ²³²Th concentrations in the soil were 3.63 and 43.00 ppm, respectively. The average terrestrial gamma-ray dose rate was found to be 200 nGy h⁻¹.

Siak *et al.* (2009) measured the natural background gamma-radiation and radioactivity concentrations in Kinta District, Perak, Malaysia using an HPGe detector and a NaI (TI) survey meter. The gamma-ray dose rate was 222 nGy h⁻¹ and the ²³⁸U, ²³²Th, and ⁴⁰K concentrations in the soil ranged from 12 Bq kg⁻¹ to 426 Bq kg⁻¹, 19 Bq kg⁻¹ to 1377 Bq kg⁻¹, and < 19 Bq kg⁻¹ to 2204 Bq kg⁻¹, respectively.

Malain *et al.* (2010) determined the naturally occurring radioactive materials in beach sand along the Andaman Coast of Thailand by using an HPGe detector. The concentrations of ²²⁶Ra, ²³²Th, and ⁴⁰K were found to range from 2.7 Bq kg⁻¹ to 23.5 Bq kg⁻¹, 3.0 Bq kg⁻¹ to 34.6 Bq kg⁻¹ and 10.7 Bq kg⁻¹ to 654.3 Bq kg⁻¹, respectively. The gamma-ray dose rate was found to be 31 nGy h⁻¹.

Santawamaitre *et al.* (2011) determined the activity concentrations of radionuclides in the ²³⁸U and ²³²Th decay chains and from ⁴⁰K in the soil along the Chao Phraya river in Thailand using HPGe spectrometry. The activity concentrations of ²³⁸U, ²³²Th, and ⁴⁰K were found to be 60, 65, and 432 Bq kg⁻¹, respectively. The gamma-ray dose rate in air was 85 nGy h⁻¹.

Huy & Luyen (2006) measured the radioactivity concentrations of ^{226}Ra (29 Bq kg^{-1}), ^{232}Th (51 Bq kg^{-1}), and ^{40}K (293 Bq kg^{-1}) for soil in Southern, Vietnam by using an HPGe detector. The gamma-ray dose rate in air was 55 nGy h^{-1} .

Alam *et al.* (1999a) measured the specific activity of ^{222}Rn , ^{226}Ra , ^{232}Th and ^{40}K in the drinking water of the Chittagong region of Bangladesh by HPGe spectrometry.

^{222}Rn concentration in the drinking water was 4 Bq l^{-1} . The mean specific activities of ^{226}Ra , ^{232}Th , and ^{40}K were 0.043, 0.19, and 4 Bq l^{-1} , respectively. No ^{134}Cs and ^{137}Cs activities were detected.

Alam *et al.* (1999b) measured the radioactivity of ^{226}Ra , ^{232}Th , and ^{40}K in beach sand and soils from the tourist zone of Cox's Bazar, Bangladesh by using an HPGe detector. The average activities of ^{226}Ra , ^{232}Th , and ^{40}K in the soils were 19, 37, and 458 Bq kg^{-1} , respectively. The corresponding values for the sand were 1346, 2485, and 570 Bq kg^{-1} , respectively. The gamma-ray dose rate in air was 52 nGy h^{-1} .

Yang *et al.* (2005) studied the natural radioactivity of soils at the Xiazhuang granite area in China by using an HPGe detector. The activities of ^{238}U , ^{232}Th , and ^{40}K were found to be 112, 72, and 672 Bq kg^{-1} , respectively. The gamma-ray dose rate was 124 nGy h^{-1} .

Song *et al.* (2012) measured the concentrations of natural radionuclides ^{238}U (140 Bq kg^{-1}), ^{226}Ra (134 Bq kg^{-1}), ^{232}Th (187 Bq kg^{-1}), and ^{40}K (680 Bq kg^{-1}) in soil in Guangdong, China by using HPGe spectrometry. The outdoor gamma-ray dose rates calculated from the activity concentrations of ^{226}Ra , ^{232}Th , and ^{40}K were found to have a mean value of 165 nGy h^{-1} .

Tahir *et al.* (2005) measured the activity concentrations of naturally occurring radionuclides in soil from Punjab Province in Pakistan by using a HPGe detector.

The mean activity concentrations for ^{232}Th , ^{226}Ra , and ^{40}K were found to be 41, 35, and 615 Bq kg⁻¹, respectively. The gamma-ray dose rate in air was 68 nGy h⁻¹.

Tufail *et al.* (2006) measured the terrestrial radiation to assess the gamma-ray dose in soils of Faisalabad, Pakistan by using a HPGe detector. Activity concentration levels due to ^{226}Ra , ^{232}Th , ^{137}Cs , and ^{40}K were found to be 30, 56, 4, and 602 Bq kg⁻¹, respectively. The gamma-ray dose rate in air was 73 nGy h⁻¹.

Mujahid & Hussain (2010) measured the natural radioactivity in soil in Baluchistan Province, Pakistan by using a HPGe detector. The concentrations of ^{226}Ra , ^{232}Th , and ^{40}K were ranged from 15 Bq kg⁻¹ to 27 Bq kg⁻¹, 20 Bq kg⁻¹ to 37 Bq kg⁻¹, and 328 Bq kg⁻¹ to 648 Bq kg⁻¹, respectively. The dose rate in air ranged from 35 nGy h⁻¹ to 59 nGy h⁻¹.

Khodashenas *et al.* (2012) found the concentration of naturally occurring radioactive materials of soil in the southwestern oil wells of Iran by using a HPGe detector. The ^{232}Th and ^{40}K concentrations in the soil samples were determined, and ^{226}Ra in both soil and water was analyzed. The concentration of ^{232}Th ranged from 9 Bq kg⁻¹ to 403 Bq kg⁻¹, whereas that of ^{40}K ranged from 82 Bq kg⁻¹ to 815 Bq kg⁻¹.

Very low concentrations of ^{226}Ra from 11 Bq kg⁻¹ to 42 Bq kg⁻¹ were indicated, except for the rare instances when concentrations of 282, 602, and 1480 Bq kg⁻¹ were observed. ^{226}Ra concentration in water ranged from 0.1 Bq l⁻¹ to 30 Bq l⁻¹.

Ahmad & Hussein (1998) determined the natural radioactivity of ^{226}Ra (54 Bq kg⁻¹), ^{232}Th (24 Bq kg⁻¹), and ^{40}K (488 Bq kg⁻¹) in soil and ^{226}Ra (25 Bq kg⁻¹), ^{232}Th (15 Bq kg⁻¹), and ^{40}K (188 Bq kg⁻¹) in sand samples collected throughout Jordan by using an HPGe detector.

Saqan *et al.* (2001) measured the activities of natural radioactive isotopes and calculated the concentrations of the parents of their natural radioactive series in water

in Ma'in, Himma, Al-Shona, Afra and Barbeita in Jordan by HPGe spectrometry. The radionuclides were ^{234}Th , ^{226}Ra , ^{214}Pb , ^{214}Bi , ^{228}Ac , ^{228}Th , ^{212}Pb , ^{212}Bi , ^{208}Tl , ^{235}U , and ^{40}K . The activities ranged from 0.14 Bq l⁻¹ to 35.0 Bq l⁻¹, whereas the concentrations of the parent ^{238}U and ^{232}Th isotopes ranged from 0.003 mg l⁻¹ to 0.59 mg l⁻¹.

Al-Kharouf *et al.* (2008) measured the natural radioactivity of soil in Khan Al-Zabeeb, Jordan by HPGe spectrometry. The concentrations of ^{238}U , ^{235}U , ^{226}Ra , ^{222}Rn , ^{232}Th , ^{137}Cs , and ^{40}K were found to be 70, 5, 339, 266, 41, 2, and 228 Bq kg⁻¹, respectively. The gamma-ray dose rate in air was 54 nGy h⁻¹.

Al-Hamarneh & Awadallah (2009) determined the radioactivity of soil in the highlands of northern Jordan by using an HPGe detector. The gamma-ray dose rate in the study area was found to be 52 nGy h⁻¹, and the total average concentrations of radionuclides ^{226}Ra , ^{238}U , ^{232}Th , and ^{40}K were 43, 50, 27, and 291 Bq kg⁻¹, respectively.

Sahin & Cavas (2008) measured the natural radioactivity of soil in central Kutahya, Turkey by using a NaI (TI) scintillation detector. The ^{238}U , ^{232}Th , and ^{40}K concentrations were 33, 32, and 255 Bq kg⁻¹, respectively. The gamma-ray dose rate was 46 nGy h⁻¹.

Belivermis *et al.* (2010) determined the natural radionuclide levels of the soil in Istanbul, Turkey by using an HPGe detector. The average activity concentrations of ^{232}Th , ^{238}U , ^{40}K were 32, 27, and 393 Bq kg⁻¹, respectively. The gamma-ray dose rate was 49 nGy h⁻¹.

Abd El-Mageed *et al.* (2011) measured the natural radioactivity levels of ^{226}Ra , ^{232}Th , and ^{40}K (44, 58, and 823 Bq kg⁻¹, respectively) and the fallout of ^{137}Cs (5 Bq

kg⁻¹) in the soil sample from Juban, Yemen by using an HPGe detector. The gamma-ray dose rate in air was 89 nGy h⁻¹.

The natural radioactivity of gamma-ray and the radon concentrations of the soil in Southern Egypt were measured by gamma-ray spectroscopy equipped with an HPGe detector and a solid-state nuclear track detector (SSNTD) (CR-39). The ²³⁸U, ²³²Th, and ⁴⁰K concentrations were found to be 19, 6, and 433 Bq kg⁻¹, respectively. The radon concentrations varied from 2 Bq kg⁻¹ to 5 Bq kg⁻¹ (Sroor *et al.*, 2001).

Ahmed & El-Arabi (2005) measured the natural radioactivity concentration of ²²⁶Ra, ²³²Th, and ⁴⁰K in soil in Upper Egypt by HPGe spectrometry. The average values of ²²⁶Ra were 14 and 12 Bq kg⁻¹, respectively. The average values of ²³²Th were 12 and 11 Bq kg⁻¹, respectively, and those of ⁴⁰K were 1233 and 1636 Bq kg⁻¹, respectively.

Osman *et al.* (2008) analyzed the surface water and groundwater for ²³⁸U, ²²⁶Ra, ²²²Rn, and ²³²Th concentrations in Kadugli, Sudan by using a NaI (TI) detector. The surface water showed very low levels of radionuclide concentrations: < 1.0 mBq l⁻¹ to 7.5 mBq l⁻¹, 8.5 mBq l⁻¹ to 16.5 mBq l⁻¹, < 1.6 mBq l⁻¹, and < 0.1 mBq l⁻¹ to 0.39 mBq l⁻¹ for ²³⁸U, ²²⁶Ra, ²²²Rn, and ²³²Th, respectively. The corresponding values for groundwater were 16 mBq l⁻¹ to 1720 mBq l⁻¹, 8 to 14 mBq l⁻¹, 3000 mBq l⁻¹ to 139,000 mBq l⁻¹, and < 0.1 mBq l⁻¹ to 39 mBq l⁻¹, respectively.

Ngachin *et al.* (2008) determined the radioactivity levels of soils in the Southwest Region of Cameroon by HPGe spectrometry. The ²²⁶Ra, ²³²Th, and ⁴⁰K concentrations in the soils ranged from 11 Bq kg⁻¹ to 17 Bq kg⁻¹, 22 Bq kg⁻¹ to 36 Bq kg⁻¹, and 43 Bq kg⁻¹ to 201 Bq kg⁻¹, respectively. ¹³⁷Cs was found to have a low concentration. The outdoor gamma-ray dose rate calculated from the activity concentrations was found to be 29 nGy h⁻¹.

Using a HPGe detector, Arogunjo *et al.* (2009) determined the activity concentrations of ^{238}U and ^{232}Th in soil and water samples collected from a Nigerian tin mining area of Bisichi, Nigeria. The ^{238}U and ^{232}Th concentrations in the soil sample ranged from 9 kBq kg⁻¹ to 51 kBq kg⁻¹ and 17 kBq kg⁻¹ to 98 kBq kg⁻¹, respectively. The ^{238}U and ^{232}Th concentrations in water ranged from 0.05 mBq kg⁻¹ to 3.28 mBq kg⁻¹, and < 0.002 mBq kg⁻¹ to 0.252 mBq kg⁻¹, respectively.

With a HPGe detector, Agbalagba & Onoja (2011) evaluated the natural radioactivity levels in soil and water in four flood plain lakes in Niger Delta, Nigeria. The profiles of the radionuclides showed low activity in the study area. The average activity levels of the natural radionuclides ^{226}Ra , ^{232}Th , and ^{40}K in soil were 18, 22, and 210 Bq kg⁻¹, respectively. The corresponding values in water were 12, 12, and 97 Bq l⁻¹, respectively. The gamma-ray dose rate in air was 30 nGy h⁻¹.

Studies on the concentrations of primordial radionuclides in soil samples from southeastern Botswana were conducted using a HPGe detector. The activities of ^{226}Ra , ^{232}Th , and ^{40}K were found to be 35, 42, and 433 Bq kg⁻¹, respectively. The gamma-ray dose rate was found to be 59 nGy h⁻¹ (Murty & Karunakara, 2008).

Using a HPGe detector, Popovic *et al.* (2008) determined the concentrations of radionuclides ^{40}K (629 Bq kg⁻¹), ^{137}Cs (64 Bq kg⁻¹), ^{210}Pb (50 Bq kg⁻¹), ^{226}Ra (6 Bq kg⁻¹), ^{232}Th (48 Bq kg⁻¹), ^{235}U (6 Bq kg⁻¹), and ^{238}U (100 Bq kg⁻¹) in Borovac, Southern Serbia.

Dragović *et al.* (2012) surveyed the radium activity concentrations in the well and spring waters of Southern Serbia by HPGe detector. The mean activity concentrations of ^{226}Ra in well and spring waters were 0.36 and 0.57 Bq l⁻¹, respectively. Crystalline rocks and carbon dioxide rich-aquifers were reported to contain the highest radionuclide concentrations (up to 17 Bq l⁻¹).

Papp *et al.* (2002) determined the activity concentrations of ^{238}U , ^{226}Ra , ^{232}Th , ^{137}Cs , and ^{40}K in soil samples from Ajka, Hungary by Ge (Li) spectrometry. The concentrations in the soils samples ranged from 0 Bq kg⁻¹ to 944 Bq kg⁻¹, 16 Bq kg⁻¹ to 883 Bq kg⁻¹, 12 Bq kg⁻¹ to 43 Bq kg⁻¹, 0 Bq kg⁻¹ to 150 Bq kg⁻¹ and 146 Bq kg⁻¹ to 596 Bq kg⁻¹ for ^{238}U , ^{226}Ra , ^{232}Th , ^{137}Cs and ^{40}K , respectively.

Wallova *et al.* (2012) determined the activity concentrations of anthropogenic ^{137}Cs and natural radionuclides ^{238}U , ^{232}Th , ^{40}K , and ^{210}Pb in soil in Austria (Styria, Carinthia, and Salzburg) by reverse electrode Ge detection. The concentrations of ^{40}K , ^{238}U , ^{232}Th , ^{137}Cs , and ^{210}Pb ranged from 230 Bq kg⁻¹ to 709 Bq kg⁻¹, 22 Bq kg⁻¹ to 45 Bq kg⁻¹, 30 Bq kg⁻¹ to 46 Bq kg⁻¹, 14 Bq kg⁻¹ to 106 Bq kg⁻¹, and 70 Bq kg⁻¹ to 2051 Bq kg⁻¹, respectively.

Perrin *et al.* (2006) determined the distribution of radioelements K, U, Th, and Cs in the soils of the Hyrome watershed in France by using a Ge(Li)-HP detector. The average activities of ^{238}U , ^{232}Th , ^{137}Cs , and ^{40}K were 46, 56, 3 Bq kg⁻¹, and 997 Bq kg⁻¹, respectively. The gamma-ray dose rate in air was 85 nGy h⁻¹.

The radionuclide levels in the soil samples from Donegal, Ireland were determined using an HPGe detector. The average activity concentrations of ^{238}U , ^{226}Ra , ^{228}Ra , and ^{40}K were 79, 104, 35, and 526 Bq kg⁻¹, respectively. The highest activity occurred in the granite area, thus indicating the immobility of radionuclides in organic soils (O'Dea & Dowdall, 1999).

Dowdall *et al.* (2003) evaluated the levels of gamma-ray emitting radionuclides in the terrestrial environment of Kongsfjord, Svalbard, Norway by using an HPGe detector. The average radionuclides activities of ^{238}U , ^{226}Ra , ^{232}Th , ^{40}K , and ^{137}Cs in the soils were 42, 43, 21, 283, and 35, respectively.

Alencar & Freitas (2005) measured the gamma-ray dose rates and the activity concentrations in beach sand samples in a Brazilian southeastern coastal region. A HPGe detector and a portable environmental radiation detector called TRADOS were used. The gamma-ray dose rate ranged from 62 nGy h⁻¹ to 126 nGy h⁻¹. The ²³⁸U, ²³²Th, and ⁴⁰K concentrations in the soil samples were 56, 61, and 523, respectively.

Montes *et al.* (2012) determined the concentrations of ²²⁶Ra, ²³²Th, and ⁴⁰K radionuclides in soils in Buenos Aires, Argentina by using HPGe spectrometry. The average concentrations of ²²⁶Ra, ²³²Th, and ⁴⁰K were 36, 39, and 688 Bq kg⁻¹, respectively.

Mireles *et al.* (2003) evaluated the concentrations of natural radionuclides of soil in the cities of Zacatecas and Guadalupe, Zacatecas in Mexico by HPGe spectrometry. The activity concentrations of ²²⁶Ra, ²³²Th, and ⁴⁰K varied from 11 Bq kg⁻¹ to 38 Bq kg⁻¹, 8 Bq kg⁻¹ to 38 Bq kg⁻¹, and 309 Bq kg⁻¹ to 1,049 Bq kg⁻¹, respectively. The overall population mean outdoor terrestrial gamma-ray dose rate was 45 nGy h⁻¹.

2.2.2 Radon and Thoron Measurements in Soil and Sand Samples by CR-39 and RAD7 Detection

SSNTDS (CR-39 detectors) are used for long-term monitoring of the concentrations of radon and thoron. The portable detector, RAD7, is a versatile instrument and can form the basis of a comprehensive ²²²Rn and ²²⁰Rn measurement system.

Mahat *et al.* (1993) developed a dosimeter for the measurement of radon emanation rate from soils in hot, wet, and humid weather condition in Malaysia by using an (SSNTD) at 75 cm depth.